Solvent effects on the redox properties of ferrocenoyl-dipeptides

Murray V. Baker,[a] Heinz-Bernhard Kraatz*[b] and J. Wilson Quail[b]

[a] *Department of Chemistry, The University of Western Australia, Crawley, WA 6907, Australia*
[b] *Department of Chemistry, 110 Science Place, University of Saskatchewan, Saskatoon, SK S7N 5C9, Canada. E-mail: kraatz@skyway.usask.ca; http.//www.usask.ca/chemistry/kraatz.html; Fax: +1 (306) 966-4730*

Received (in Gainesville, FL, USA) 23rd June 2000, Accepted 8th December 2000
First published as an Advance Article on the web 14th February 2001

The preparation and characterization of the novel ferrocenoyl-dipeptides, Fc-Asp(OBzl)-Asp(OBzl)-OBzl (**5**), Fc-Asp(OBzl)-Glu(OEt)-OEt (**6**) and Fc-Asp(OBzl)-Cys(Bzl)-OMe (**7**) are reported. In addition, Fc-Asp(OBzl)-OBzl (**4**) and its free acid, Fc-Asp(OH)-OH (**8**), were prepared. A crystal structure determination of **8** revealed an extensive H-bonding network involving a solvent molecule and adjacent molecules of **8** and suggests that these complexes are able to form strong hydrogen bonds with solvent molecules. All compounds show reversible one-electron oxidations in solution. The half-wave potential is strongly influenced by the nature of the solvent and correlates with the hydrogen donor ability α of the Kamlet–Taft formalism.

The redox potential of ferrocenoyl-peptides (Fc-peptides) has been shown to be sensitive to changes in the length and primary structure of the peptide chain, and, perhaps more importantly, the secondary structure of the peptide chain.[1] Furthermore, H-bonding interactions between substrates such as 3-aminopyrazole (3-apzl) derivatives and the peptide backbone have been detected electrochemically.[2] Importantly, substrate binding was found to be directly related to the rigidity of the peptide and to the nature of the solvent.[3] Interactions between the substrate and the peptide backbone occurred only in non-polar and non-protic solvents, which could not compete with H-bonding sites on the backbone. Polar solvents prevented substrate binding completely.

These solvent effects prompted us to investigate the redox behavior of Fc-dipeptides in various solvents in more detail. Our findings may help to further the understanding of peptide secondary structure, but in a much broader context, may help to improve understanding of the effects of "solvation" on biological redox centers. For example, both high and low potential [4Fe-4S] iron–sulfur proteins contain the structurally robust iron–sulfur cubane cluster linked to the protein through iron–cysteine thiolate linkages.[4] In view of the structural similarity of clusters in these proteins, the reason for the dramatic difference in redox potential between HiPIP (high potential iron proteins) and other [4Fe-4S]-ferredoxins is not apparent. Changes in the immediate non-coordinative environment of the [4Fe-4S]-cluster may explain these redox variations. Studies of a series of blue copper proteins by Loppnow and co-workers have shown that the protein environment, which was not involved in coordination to the copper ion, caused strong variations in the electronic properties of the redox site.[5]

Whereas the aqueous solvation of peptides[6–8] and redox proteins[9] has received significant attention, the effects of solvation on simple redox-labeled peptides has not been studied. On the other hand, solvent effects of ferrocenes and modified ferrocenes have received wide attention due to their importance as accepted standards in electrochemical experiments and their wide use in biological receptor systems. The ferrocene/ferrocenium couple has been recognized as having an electrode potential that varies little with solvent (THF, DMF, MeCN, DMSO, and MeOH).[10] More recently, Blackburn and Hupp showed that the redox potential of ferrocene depends on the degree of association of the ferrocenium cation with the counterion and its activity in a particular solvent.[11a] Building on these results, Lay and coworkers have reported a detailed study of solvation of ferrocene and decamethylferrocene.[11b] Direct interactions of the solvent with the iron center and/or the cyclopentadienyl rings appear responsible for the large solvent dependence of the reduction potential of ferrocene and its permethylated derivative and have been correlated to solvation parameters first described by Kamlet *et al.*[12] The Kamlet–Taft linear solvation energy relationship (LSER)[12] has been successfully applied by them and others to describe a variety of properties, such as the rate of a reaction, the free energy and enthalpy of solvation and the solubility.[12–14]

In the context of ferrocene-based receptors,[15] calix[4]arene-modified ferrocenes exhibit a significant solvent dependence, with the solvent being able to alter the anion recognition properties of the receptor. In general, the binding constants correlated well with solvent parameters, such as the relative permittivity ε, the solvent dipole moment μ, and Gutmann's acceptor number AN.[15e]

In this study, we have prepared four novel ferrocenoyl-peptides, characterized them fully and investigated their redox properties in various solvents. Each dipeptide contains an asparate residue directly bound to the ferrocenoyl group with a second amino acid residue bound to the aspartate residue. These short dipeptides are unable to adopt a stable secondary structure. It was expected that in these dipeptides, the second amino acid residue will not have any significant influence on the redox properties of the ferrocenoyl moiety, but that the interaction of solvent molecules with the amide NH and the carbonyl of the peptide backbone would be sensed by the ferrocenoyl group. In particular, it was expected that the interaction of the solvent molecules with the amide group directly attached to the ferrocene should influence the electronic properties significantly. We have used our results to explore the applicability of free solvation relationships such as the Kamlet–Taft expression to the redox properties of ferrocenoyl-dipeptides.

Experimental

General

Ferrocene carboxylic acid (Strem), 1-ethyl-3-(3-dimethylaminopropyl)carbodiimide (EDC), H-Asp(OBzl)-OBzl, H-Cys(Bzl)-OMe, Boc-Asp(OBzl)-OH, Boc-Glu(OBzl)-OH (all Advanced ChemTech), hydroxybenzotriazole (HOBt) (Aldrich) and H-Glu(OEt)-OEt (Aldrich) were used as received. For synthetic purposes, $CHCl_3$ was dried over CaH_2 and distilled prior to use. Et_3N was used without any further purification. ^1H and ^{13}C NMR spectra were recorded at 300.135 and 75.478 MHz, respectively, on a Bruker AMX 300 NMR spectrometer. All chemical shifts are reported in ppm and coupling constants (J) in Hz. $CDCl_3$ and MeCN-d_3 (Aldrich) were stored over molecular sieves (4 Å). ^1H NMR shifts are referenced to the non-deutero impurity in $CDCl_3$ (δ 7.24) or in MeCN-d_3 and are reported relative to tetramethylsilane (δ 0.00). Assignments in the ^1H and $^{13}C\{^1H\}$-NMR spectra were made using J-modulation and ^1H-^1H COSY experiments. All measurements were carried out at 293 K unless otherwise specified. Mass spectrometry was carried out on a VG Analytical 70/20 VSE instrument. Elemental analyses were obtained in-house on a Perkin–Elmer 2400 CHN elemental analyzer.

General procedure for the synthesis of Boc-dipeptides

Preparation and spectroscopic characterization of Boc-Asp(OBzl)-Asp(OBzl)-OBzl (1). To a cooled (−0 °C) solution of Boc-Asp(OBzl)-OH (320 mg; 1 mmol) in CH_2Cl_2 (20 mL), solid HOBt (150 mg; 1.1 mmol) and solid EDC (210 mg; 1.1 mmol) were added. After 5 min, a clear solution of H-Asp(OBzl)-OBzl · HCl (500 mg; 1.03 mmol) in CH_2Cl_2 (5 mL) and Et_3N (1 mL) were added. After overnight stirring at room temperature, the reaction mixture was extracted with saturated aqueous $NaHCO_3$ solution, followed by 10% citric acid, saturated aqueous $NaHCO_3$ solution and finally distilled water. The clear organic phase was then dried over anhydrous Na_2SO_4, filtered and pumped to dryness to give a colorless oil. Yield: 432 mg, 70%. MW for $C_{34}H_{38}N_2O_9$: calc. 618, found 619 $[M + 1]^+$; HR-MS: calc. 619.2656 $[M + 1]^+$, found 619.2656. ^1H-NMR (δ, $CDCl_3$): 7.44 (1H, d, $J_{HH} = 8.4$, NH of Asp-2), 7.34 (15H, m, aromatic H of Ph), 5.59 (1H, d, $J_{HH} = 8.2$, NH of Boc-Asp-1), 5.14 (2H, s, CH_2Ph), 5.12 (2H, s, CH_2Ph), 5.07 (2H, apparent doublet, CH_2Ph), 4.88 (1H, dt, $J_{HH} = 8.1$, $J_{HH} = 4.5$, CH), 3.88 (1H, m, CH), 3.10–2.67 (4H, m, diastereotopic H of $CH_2COOBzl$). $^{13}C\{^1H\}$-NMR (δ, $CDCl_3$): 170.8, 170.5, 170.3, 169.9 (all C=O), 162.3 (Boc C=O), 135.4, 135.3, 135.0, 128.5, 128.3, 128.2, 128.1, 127.7, 127.5, 126.8 (all C of Ph), 67.4 (–OCH_2Ph), 67.0 (–OCH_2Ph), 66.7 (–OCH_2Ph), 66.5 [$Me_3CC(O)$ of Boc], 51.2 (C_α of Asp-1), 48.8 (C_α of Asp-2), 38.7 (–CH_2 of Asp-1), 36.0 (–CH_2 of Asp-2), 28.1 (CH_3 of Boc).

Spectroscopic characterization of Boc-Asp(OBzl)-Glu(OEt)-OEt (2). Yield: 290 mg, 57%. MW for $C_{25}H_{36}N_2O_9$: calc. 508, found 509 $[M + 1]^+$; HR-MS: calc. 509.2499 $[M + 1]^+$, found 509.2497. ^1H-NMR (δ, $CDCl_3$): 7.35 (5H, m, Ph), 7.13 (1H, d, $J_{HH} = 7.7$, NH of Glu), 5.68 (1H, d, $J_{HH} = 8.6$, NH of Asp), 5.14 (2H, apparent doublet, CH_2Ph), 4.56 (2H, m, CH of Asp and CH of Glu), 4.18 (2H, q, $J_{HH} = 7.3$, CH_2CH_3), 4.13 (2H, q, $J_{HH} = 7.3$, CH_2CH_3), 3.08 (1H, dd, $J_{HH} = 17.2$, $J_{HH} = 4.4$, H of the diastereotopic CH_2 of Asp), 2.72 (1H, dd, $J_{HH} = 17.2$, $J_{HH} = 5.9$, H of the diastereotopic CH_2 of Asp), 2.37 (2H, q, $J_{HH} = 7.6$, $CHCH_2CH_2CO_2$ of Glu), 2.23 (1H, m, $CHCHHCH_2CO_2$ of Glu), 1.98 (1H, m, $CHCHHCH_2CO_2$ of Glu), 1.46, [9H, s, $C(CH_3)_3$]. $^{13}C\{^1H\}$-NMR (δ, $CDCl_3$): 172.9, 172.0, 171.5, 170.9 (all C=O), 155.6 (Boc C=O), 135.6, 128.8, 128.6, 128.5 (all C of Ph), 80.8 [$C(CH_3)_3$], 67.1 (CH_2Ph), 61.8 (CH_2CH_3), 60.8 (CH_2CH_3), 52.0 and 50.8 (CH), 36.3 and 30.3 CH_2, 28.5 [$C(CH_3)_3$], 27.6 (CH_2), 14.4 (CH_2CH_3), 14.3 (CH_2CH_3).

Spectroscopic characterization of Boc-Asp(OBzl)-Cys(Bzl)-OMe (3). Yield: 441 mg, 83%. MW for $C_{27}H_{35}N_2O_7S$: calc. 530, found 531 $[M + 1]^+$; HR-MS: calc. 531.2165 $[M + 1]^+$, found 531.2154. ^1H-NMR (δ, $CDCl_3$): 7.38–7.21 (11H, m, 2 × Ph and Cys-NH), 5.72 (1H, d, $J_{HH} = 8.1$, NH of Asp), 5.14 (2H, AB multiplet, $J_{HH} = 12.3$, CH_2Ph), 4.75 (1H, dt, $J_{HH} = 7.8$, $J_{HH} = 5.6$, CH of Asp), 4.60 (1H, br m, CH of Cys), 3.72 (3H, s, OCH_3), 3.71 (2H, s, SCH_2Ph), 3.05 (1H, dd, $J_{HH} = 17.2$, $J_{HH} = 4.5$, H of the diastereotopic CH_2 of Asp), 2.86 (2H, m, $CHCH_2S$), 2.75 (1H, dd, $J_{HH} = 17.2$, $J_{HH} = 6.0$, H of the diastereotopic CH_2 of Asp), 1.47 [9H, s, $C(CH_3)_3$]. $^{13}C\{^1H\}$-NMR (δ, $CDCl_3$): 171.8, 171.0, 170.9 (all C=O), 155.7 (Boc C=O), 137.9, 135.6, 129.2, 128.8, 128.6, 128.5, 127.5 (all C of 2 × Ph), 80.8 [$C(CH_3)_3$], 67.1 (OCH_2Ph), 52.8 (CH_3), 52.2 and 50.8 (CH), 36.7, 36.3, 33.3 (all CH_2), 28.5 [$C(CH_3)_3$].

Peptide coupling to ferrocene carboxylic acid

Preparation and spectroscopic characterization of Fc-Asp(OBzl)-OBzl (4). The coupling of H-Asp(OBzl)-OBzl to FcCOOH was carried out as described above for **1**, on a 1 mmol scale. Yield: 454 mg; 86%. MW for $C_{29}H_{27}NO_5Fe$: calc. 525, found (FAB) 525 $[M]^+$; HR-MS (FAB): calc: 525.1239, found 525.1246. ^1H-NMR (δ, $CDCl_3$): 7.36 (10H, m, aromatic H of Ph), 6.80 (1H, d, $J_{HH} = 8.1$, NH), 5.22 (2H, s, CH_2Ph), 5.07 (2H, m, CH_2Ph), 5.06 (1H, m, H_α of Asp), 4.71 (1H, s, H_o of subst. Cp), 4.58 (1H, s, H_o of subst. Cp), 4.35 (2H, m, H_m of subst. Cp), 4.19 (5H, s, unsubst. Cp), 3.19 (1H, dd, $J_{HH} = 17.2$, $J_{HH} = 4.4$, diastereotopic H of CH_2 of Asp), 2.98 (1H, $J_{HH} = 17.2$, $J_{HH} = 4.5$, diastereotopic H of CH_2 of Asp). $^{13}C\{^1H\}$-NMR (δ, $CDCl_3$): 170.8, 170.6, 170.2 (all C=O), 135.2 (C_{ipso} Ph), 135.1 (C_{ipso} Ph), 128.6, 128.5, 128.4, 128.3, 128.2, 127.7, 126.8, 127.5, 127.4 (all C of Ph), 74.7 (C_{ipso} of subst. Cp), 70.6, 70.5 (both C_{meta} of subst. Cp), 69.7 (C of unsubstituted Cp), 68.4, 67.9 (both C of subst. Cp), 67.5 (–OCH_2Ph), 66.7(–OCH_2Ph), 48.4 (CH of Asp), 36.5 (–$CH_2COOBzl$). $E_{1/2} = 216$ mV (*vs.* Fc/Fc^+; peak width 95 mV). λ_{max} nm (ε/dm^3 mol^{-1} cm^{-1}) = 444 (1200).

Spectroscopic characterization of Fc-Asp(OBzl)-Asp(OBzl)-OBzl (5). On the 0.55 mmol scale, yield: 389 mg; 97%. HR-MS (EI): calc. for $C_{40}H_{38}N_2O_8Fe$ 730.1977, found 730.1984. ^1H-NMR (δ, $CDCl_3$): 7.58 (1H, d, $J_{HH} = 8.2$, NH of Asp-2), 7.35 (15H, m, aromatic H of Ph), 6.94 (1H, d, $J_{HH} = 8.3$, NH of Fc-Asp-1), 5.15 (2H, s, OCH_2Ph), 5.13 (2H, s, OCH_2Ph), 5.10 (2H, s, OCH_2Ph), 4.96 (1H, m, CH of Asp), 4.92 (1H, dt, $J_{HH} = 8.2$, $J_{HH} = 4.4$, CH of Asp), 4.70 (1H, m, H_o of subst. Cp), 4.64 (1H, m, H_o of subst. Cp), 4.37 (2H, s, H_m of subst. Cp), 4.21 (5H, s, unsubst. Cp), 3.20–2.71 (4H, m, diastereotopic H of CH_2 of Asp). $^{13}C\{^1H\}$-NMR (δ, $CDCl_3$): 172.3, 170.9, 170.8, 170.7, 170.2 (all C=O), 135.6, 135.5, 135.3, 128.8, 128.7, 128.6, 128.5 (all C of Ph), 75.1 (quaternary C of subst. Cp), 71.0, 71.9 (both are C of subst. Cp), 70.1 (C of unsubst. Cp), 68.8, 68.2 (both are C of subst. Cp), 67.8 (–OCH_2Ph), 67.2 (–OCH_2Ph), 67.1 (–OCH_2Ph), 49.3 (–CH– of Asp-1), 49.2 (–CH– of Asp-2), 36.3 (–CH_2– of Asp-1), 36.2 (–CH_2– of Asp-2). $E_{1/2} = 194$ mV (*vs.* Fc/Fc^+; peak width 70 mV; in MeCN). λ_{max}/nm (ε/dm^3 mol^{-1} cm^{-1}) = 442 (1500).

Spectroscopic characterization of Fc-Asp(OBzl)-Glu(OEt)-OEt (6). Yield: 890 mg, 72% (2 mmol scale). HR-MS (EI): calc. for $C_{31}H_{36}N_2O_8Fe$ 620.1821, found 620.1825. ^1H-NMR (δ, $CDCl_3$): 7.35 (6H, m, Ph and overlapping peaks from NH of Glu as confirmed by ^1H-^1H COSY NMR), 7.06 (1H, d, $J_{HH} = 8.3$, NH of Asp), 5.17 (2H, s, OCH_2Ph), 5.00 (1H, m, CH of Asp), 4.73 (2H, m, H_o of subst. Cp), 4.57 (1H, m, CH of Glu), 4.37 (2H, apparent triplet, $J_{HH} = 1.9$, H_m of Cp), 4.20 (5H, s, H of subst. Cp), 3.16 (1H, dd, $J_{HH} = 17.1$, $J_{HH} = 4.4$, H

Table 1 Crystal data and structure refinement for $\mathbf{8}\cdot 1/3H_2O$

Empirical formula	$C_{15}H_{15}FeNO_5\cdot 0.33H_2O$
Formula weight	351.10
T/K	123(2)
Crystal system	Monoclinic
Space group	$P2_1$
a/Å	7.455(3)
b/Å	10.0294(13)
c/Å	10.568(5)
α/°	90
β/°	109.20(2)
γ/°	90
U/Å^3	746.2(5)
Z	2
μ/mm^{-1}	1.036
Reflections collected	4589
Independent reflections	2384 [R(int) = 0.0216]
Reflections observed [$I > 2\sigma(I)$]	2152
Final R indices [$I > 2\sigma(I)$]	$R_1 = 0.0216$, $wR_2 = 0.0544$
R indices (all data)	$R_1 = 0.0296$, $wR_2 = 0.0565$

of the diastereotopic CH_2 of Asp), 2.76 (1H, dd, $J_{HH} = 17.1$, $J_{HH} = 6.1$, H of the diastereotopic CH_2 of Asp), 2.41 (2H, m, diastereotopic H of $CH_2CH_2CO_2$ of Glu), 2.22 (1H, m, diastereotopic H of $CH_2CH_2CO_2$ of Glu), 2.01 (1H, m, diastereotopic H of $CH_2CH_2CO_2$ of Glu). $^{13}C\{^1H\}$-NMR (δ, $CDCl_3$): 173.0, 172.2, 171.4, 170.9, 170.8 (all C=O), 135.5, 128.8, 128.6, 128.5 (all C of Ph), 75.0 (C_{ipso} of subst. Cp), 70.9 (C of subst. Cp), 70.0 (C of unsubst. Cp), 68.6, 68.4 (both C of subst. Cp), 67.1 (OCH_2Ph), 61.8 (OCH_2CH_3), 60.9 (OCH_2CH_3), 52.3 (CH of Glu), 49.3 (CH of Asp), 36.1, 30.4, 27.2 (all CH_2), 14.3, 14.3 (both CH_3 of Et). λ_{max}/nm (ε/dm^3 mol^{-1} cm^{-1}) = 440 (1100).

Spectroscopic characterization of Fc-Asp(OBzl)-Cys(Bzl)-OMe (7). Yield: 39% (2 mmol scale reaction) after chromatography (silica 200 mesh, EtOAc–hexanes 1 : 1). Anal. calc. for $C_{33}H_{34}N_2O_6SFe$: C 61.69, H 5.33, N 4.36; found C 62.03, H 5.25, N 4.12%. MW for $C_{33}H_{34}N_2O_6SFe$: calc. 642, found 642 $[M]^+$; HR-MS: calc. 642.1487 $[M]^+$, found 642.1494. ^{1}H-NMR (δ, $CDCl_3$): 7.52 (1H, d, $J_{HH} = 7.8$, Cys-NH), 7.21–7.37 (10H, m, 2 × Ph), 7.19 (1H, d, $J_{HH} = 8.5$, Asp-NH), 5.17 (2H, s, OCH_2), 5.09 [1H, dt, $J_{HH} = 8.0$ (doublet splitting), $J_{HH} = 5.4$ (triplet splitting), CH of Asp], 4.77 [1H, dt, $J_{HH} = 7.8$ (doublet splitting), $J_{HH} = 5.7$ (triplet splitting), CH of Cys], 4.71 (1H, apparent q, splitting 1.6, 1 × Cp-H), 4.69 (1H, apparent q, splitting 1.5, 1 × Cp-H), 4.34 (2H, apparent t, splitting 1.9, 2 × Cp-H), 4.20 (5H, s, 5 × Cp-H), 3.70 (2H, s, SCH_2Ph), 3.68 (3H, s, OCH_3), 3.14 (1H, dd, $J_{HH} = 16.8$, $J_{HH} = 4.8$, diastereotopic H of CH_2 of Asp), 2.8–2.9 (3H, m, overlapping signals of the diastereotopic H of CH_2 of Asp and Cys-CH_2). $^{13}C\{^1H\}$-NMR (δ, $CDCl_3$): 172.0, 171.06, 171.0, 170.9 (all C=O), 137.8, 135.7, 129.2, 128.9, 128.8, 128.6, 128.55, 127.4 (all C of 2 × Ph), 75.2 (quaternary C of subst. Cp) 71.1, 71.0, 68.7, 68.6 (all methine C of subst. Cp), 70.1 (unsubst. Cp), 67.1 (CH_2), 52.9, 52.3, 49.5 (all CH), 36.7, 36.2, 33.4 (all CH_2). λ_{max}/nm (ε/dm^3 mol^{-1} cm^{-1}) = 446 (1250).

Preparation and spectroscopic characterization of Fc-Asp(OH)-OH (8). A slow stream of hydrogen gas was bubbled through a vigorously stirred mixture of Fc-Asp(OBzl)-OBzl (**4**) (195 mg, 0.37 mmol) and 5% Pd/C (0.1 g) in MeOH (40 ml). The reaction was monitored by TLC (silica; CH_2Cl_2) and was complete after 20 min (**8** has an $R_f = 0$). Pd/C was removed by filtration. Water (10 mL) was added and the pH of the solution was adjusted to pH 2 by addition of 1 N HCl. The product was extracted into CH_2Cl_2 (3 × 50 mL). The combined extracts were concentrated and layering with Et_2O gave the product as X-ray quality orange crystals. Yield: 95 mg, 0.27 mmol, 73%. Anal. calc. for $C_{15}H_{15}NO_5Fe$: C 52.16, H 4.38, N 4.06; found C 51.79, H 4.57, N 3.75%. MW for $C_{15}H_{15}NO_5Fe$: calc. 345, found (FAB-MS) 346 $[M + 1]^+$; HR-MS(FAB): calc. 345.0300, found 345.0301. ^{1}H-NMR (δ, MeCN-d_3): 6.95 (1H, d, $J_{HH} = 11.0$, NH), 4.78 (1H, m, H_α of Asp), 4.71 (2H, apparent t, $J_{HH} = 1.6$, H_o of subst. Cp), 4.38 (2H, apparent t, $J_{HH} = 1.9$, H_m of subst. Cp), 4.23 (5H, s, unsubst. Cp), 2.90 (2H, m, diastereotopic Hs of CH_2 of Asp). $E_{1/2} = 198$ mV (*vs.* Fc/Fc^+; peak width 75 mV).

Electrochemical studies

All electrochemical experiments were carried out using a CV-50W Voltammetric Analyzer (BAS) at room temperature (23 °C). No special precautions were taken to exclude oxygen. All solvents were dried using the appropriate drying agents (CH_2Cl_2/CaH_2; $CHCl_3/CaH_2$; MeOH/Mg; MeCN/CaH_2; acetone/Na_2SO_4/molecular sieves; MeOH/Na; EtOH/Na; ^{i}PrOH/Na; THF/Na/benzophenone) and freshly distilled prior to use. Tetrabutylammonium perchlorate (TBAP) was used as supporting electrolyte (0.1 M). For the cyclic voltammetry studies a glassy carbon working electrode (BAS, diameter 2 mm) and a platinum wire counter electrode were used. The reference electrode was an Ag/AgCl electrode (BAS). iR compensation was applied. Background scans of the solvent containing 0.1 M TBAP were collected before each set of experiments and then subtracted from the spectra.

X-Ray structural studies

Yellow–orange single crystals of Fc-Asp(OH)-OH · 1/3 H_2O(**8** · $1/3H_2O$) were obtained from a solution of CH_2Cl_2 layered with Et_2O and mounted on a glass fiber using epoxy resin. Selected crystallographic information are summarized in Table 1. Data collection proceeded at 123 K on a Nonius CAD4 diffractometer (Mo-Kα). The data were collected up to a θ limit of 30.36°, using the ω-scan mode. Of 2384 unique reflections measured, 2152 were observed [$I > 2\sigma(I)$]. Absorption correction based on a psi-scan was applied. The cell parameters were determined from 20 well-centered reflections. The structure was solved using XTAL 3.4[16a] and refined using SHELXL97.[16b] All non-hydrogen atoms were refined anisotropically. The hydrogen atoms were located in the density map and were refined with isotropic temperature factors. The occupancy for the solvent water (O100) was refined to be 0.334. The H atoms on O100 could not be found in difference maps and were not placed. The absolute configuration was determined using the Flack parameter [0.001(13)]. Weights based on statistics were used. The refinement (based on F^2_{obs}) converged to $R_1 = 0.0216$, $wR_2 = 0.0544$.

CCDC reference number 440/251. See http://www.rsc.org./suppdata/nj/b0/b005125j/ for crystallographic files in .cif format.

Results and discussion

Synthesis and characterization

Our approach to the synthesis of ferrocenoyl-dipeptides is summarized in Scheme 1. Following common peptide synthetic strategies,[17] Boc-Asp(OBzl)-OH was coupled in dichloromethane solution with H-Asp(OBzl)-OBzl · HCl, H-Glu(OEt)-OEt · HCl and H-Cys(Bzl)-OMe · HCl using EDC as a coupling reagent, to form the expected dipeptides Boc-Asp(OBzl)-Asp(OBzl)-OBzl (**1**), Boc-Asp(OBzl)-Glu(OEt)-OEt (**2**) and Boc-Asp(OBzl)-Cys(Bzl)-OMe (**3**), respectively. Removal of the Boc group and coupling of the resulting dipeptide with ferrocene carboxylic acid gave the corresponding ferrocenoyl-dipeptides Fc-Asp(OBzl)-Asp(OBzl)-OBzl (**5**), Fc-Asp(OBzl)-Glu(OEt)-OEt (**6**) and Fc-Asp(OBzl)-Cys(SBzl)-OMe (**7**) as orange oils, which solidified upon standing. As part of our study, we also prepared ferrocenoyl-aspartate-dibenzyl ester (**4**) and the corresponding free acid ferrocenoyl-aspartic acid (**8**), using similar coupling procedures.

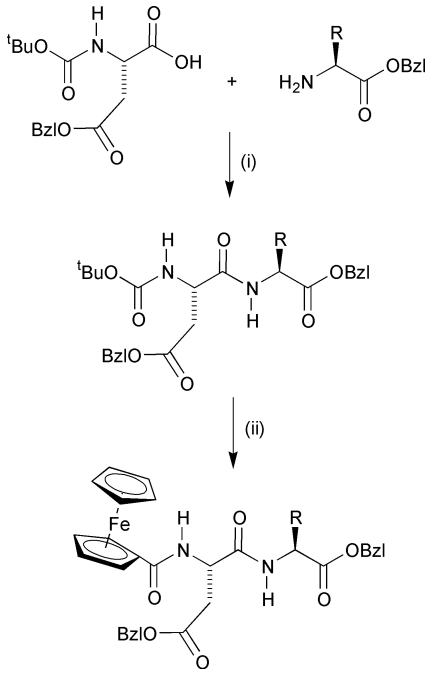

Scheme 1 General scheme for the synthesis of ferrocenoyl-dipeptides. (i) EDC, HOBt, Et_3N, CH_2Cl_2, RT; (ii) (a) TFA, CH_2Cl_2; (b) FcCOOH, EDC, HOBt, Et_3N, CH_2Cl_2, RT.

The ^{1}H-NMR spectra of deuterochloroform solutions of compounds **4**–**8** exhibit signals characteristic of mono-substituted ferrocenes, with the two signals of the two magnetically inequivalent *ortho* protons of the substituted cyclopentadienyl (Cp) ring downfield from the signal for the *meta* protons. Selected ^{1}H-NMR data are summarized in Table 2. Like all proton signals of the Cp ring, those for the *ortho* protons are observed in very narrow shift ranges, δ 4.73–4.70 and δ 4.5–4.69. In the case of Fc-Asp(OBzl)-Glu(OEt)-OEt (**6**), the signals of the two *ortho* protons are accidentally coincident. Similarly, the shifts of the signals due

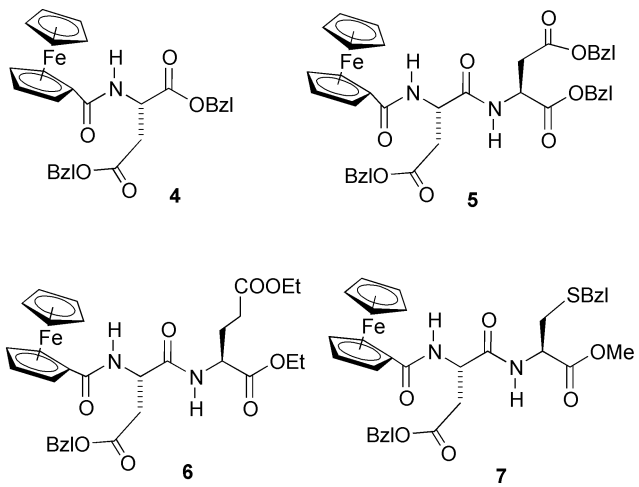

to the *meta* protons of the substituted Cp ring are essentially invariant with the peptide substituent. We would expect ^{13}C NMR to be a sensitive probe of the electronic effects in the ferrocenoyl-dipeptides. If the peptides vary the electronic properties of the Fc moiety, the *ipso*-C of the Cp ring carrying the peptide substituent should be influenced the most and its signal should be shifted significantly in the ^{13}C NMR spectrum; similar effects have been described previously for unrelated substituted aromatic systems.[18] However, signals of the *ipso*-C of the substituted Cp ring for all Fc-peptides were observed around δ 74.7–75.2, indicating only negligible electronic effects. Similarly, the visible spectra of **4**–**8** exhibit a single weak and broad absorption ($\lambda_{max} \simeq 440$ nm), characteristic of ferrocenes, which is independent of the peptide substituent. Thus, our spectroscopic results indicate that the electronic properties of the ferrocene group are not dramatically perturbed by the peptide and thus that the redox potential should be independent of the peptide substituents.

Electrochemical studies

Initial cyclic voltammograms for **4**–**7** recorded in chloroform exhibit fully reversible one-electron oxidations, as judged by the peak separation between cathodic and anodic peaks, which was in the range of 60–90 mV. In addition, the ratio of cathodic and anodic peak areas, which is also a measure of the reversibility of an electrochemical oxidation, was close to unity. All electrode potentials are reported *vs.* the Ag/AgCl reference electrode and occurred between 631 mV for **4** and 647 mV for **7** (Table 3).

Next we investigated the redox chemistry of compounds **4**–**7** in various solvents by cyclic voltammetry (CV) and found that the electrode potentials are greatly solvent dependent. The results of our CV study are summarized in Table 3. Compounds **4**–**7** exhibited fully reversible one-electron oxidation waves in most solvents with peak separations ranging from 65–85 mV, this being within the acceptable limits for reversible one-electron processes.[19] There were, however, notable exceptions where the oxidation was only quasi-reversible or even irreversible. For example, cathodic and anodic peak separations of all compounds in 1-butanol and 2-butanol were large (>200 mV) at a scan speed of 100 mV s^{-1}. At higher scan rates (above 1000 mV s^{-1}), the oxidation became fully reversible, as expected for a quasi-reversible process. Compound **7** only gave an irreversible oxidation wave in 2-pyrrolidone at 702 mV at a scan speed of 100 mV s^{-1}. This result is in line with the known redox behavior of ferrocene in strong donor solvents, such as dimethyl sulfoxide, or in the presence of anionic ligands, such as Cl^-. In both cases, irreversibility of the oxidation process was observed, presumably because the ferrocenium cation reacted rapidly with a donor species (solvent or nucleophile) to form Fe^{3+} and products of the reaction of the Cp radical with the solvent.[20]

When the solvent was changed, significant changes in the position of the halfwave potential of the ferrocenoyl-peptides **4**–**7** were observed. We were particularly interested in evaluating the redox behavior in protic solvents able to form strong

Table 2 Selected ^{1}H-NMR spectroscopic data for ferrocenoyl-peptides **4**–**7**

Compound	NH	CH_α	CH_o	CH_m	CH_{Cp}
Fc-Asp(OBzl)-OBzl (**4**)	6.80	5.06	4.71 4.58	4.35	4.19
Fc-[Asp(OBzl)]$_2$-OBzl (**5**)	7.58 (Asp-2) 6.94 (Asp-1)	4.96 4.92	4.70 4.64	4.37	4.21
Fc-Asp(OBzl)-Glu(OEt)$_2$ (**6**)	7.35 (Glu) 7.06 (Asp)	5.00 (Asp) 4.57 (Glu)	4.73	4.37	4.20
Fc-Asp(OBzl)-Cys(SBzl)-OMe (**7**)	7.52 (Cys) 7.19 (Asp)	4.77 (Cys) 5.09 (Asp)	4.71 4.69	4.34	4.20

Table 3 Halfwave potentials of Fc-Asp(OBzl)-OBzl (**4**), Fc-[Asp(OBzl)]$_2$-OBzl (**5**), Fc-Asp(OBzl)-Glu(OEt)$_2$ (**6**) and Fc-Asp(OBzl)-Cys(Bzl)-OMe (**7**) in various solvents. The solvents are grouped into (a) alcohols, (b) amides, (c) acids and (d) others and sorted by decreasing α in each group. All potentials are referenced to the potential of the Ag/AgCl reference electrode

	$E_{1/2}$/mV				
Solvent	**4**	**5**	**6**	**7**	α[12,13]
(a) Alcohols					
1,1,1-Trifluoroethanol	469	459	450	459	1.51
2-Chloroethanol	543	541	533	537	1.28
Methanol	614	622	621	623	0.98
Ethanol	658	625	649	634	0.86
1-Butanol	697	650	691	674	0.84
2-Butanol	680	655	642	665	0.79
2-Propanol	687	654	664	668	0.76
(b) Amides					
Formamide				542	0.71
N-Methylformamide				616	0.62
N-Methylacetamide				690	0.47
2-Pyrrolidone				702(irr)	0.36
(c) Acids					
Formic acid				550	1.23
Acetic acid				589	1.12
Propionic acid				621	1.12
(d) Others					
Chloroform	631	638	644	647	0.20
Acetonitrile				616	0.19
Dichloromethane	657	660	672	674	0.13
Acetone		688	683	683	0.08
Tetrahydrofuran	677	711	702	724	0.00
N,*N*-Dimethylformamide				685	0.00
Chlorobenzene				719	0.00

H-bonds with the peptide backbone, such as alcohols or amides. For example, the electrode potential for **7** exhibits a strong solvent influence on going from a non-protic to a protic solvent and shifts from 724 mV in tetrahydrofuran to 459 mV in 1,1,1-trifluoroethanol. This is a change of 265 mV and corresponds to a net stabilization of the Fe^{3+} over the Fe^{2+} oxidation state in 1,1,1-trifluoroethanol by 25.4 kJ mol^{-1}! The obvious explanation for this behavior is a change in the solvation energy between oxidized and reduced states of the ferrocene group, as was described in detail by others.[21] However, if unspecific solvation effects of the ferrocene group were solely responsible for the observed solvent effect we would expect a dependence on solvent polarity only, as was observed for ferrocene[11] and the ferrocenemethylene ammonium cation.[22] Instead, we find that the redox potentials for **4**–**7** show a dependence on the solvent's H-bond donor ability (HBD) α as defined by the Kamlet–Taft linear solvation energy relationship (LSER; *vide infra*). The electrode potentials relative to the Ag/AgCl electrode along with the α values for the solvents are given in Table 3.[13] The Kamlet–Taft LSER[12,13] has been used very successfully to express solvation effects on a range of properties, such as solubility or rates and free energies of reactions:

$$XYZ = XYZ_o + a\alpha + b\beta + s\pi^* + \cdots$$

where XYZ_o, a, and b are solvent-independent coefficients, which are characteristic of the solvation effects to be described. For some processes, many of these coefficients can be negligibly small, so that the corresponding terms are not significant in the characterization of the solvent effects for these processes. Thus, a process can be dominated by one parameter. The two solvatochromic parameters α and β are the H-bond donor ability (HBD) and the H-bond acceptor ability (HBA) of the solvent, respectively. In many cases, correlations involving the HBD ability β of the solvent show discontinuities. This has led to the introduction of an empirical "solvent family" or empirical coordinate covalency parameter ζ and the use of multilinear regression analysis in order to find the dependence on both parameters β and ζ. The ζ parameter is only used in conjunction with β. The parameter π* describes the polarity and polarizability of the solvent.

Fig. 1 shows a plot of the electrode potential for the one-electron redox process of the Fc group in **7** *vs.* the solvent's HBD ability α. Instead of a single linear relationship between E^o and α, as we would expect if E^o were to depend solely on α, we observe discontinuities, suggesting other contributing influences that are not accounted for. Attempts were made to explore the dependence of E^o on more than one Kamlet–Taft parameter. However, plots of E^o *vs.* β, π*, or α/β, β/ζ combinations do not show any correlations and produce only a scattering of points. It appears that these discontinuities may be related to the differences in interactions that exist in solution between the ferrocenoyl-dipeptides and these three groups of solvents. Protic acids and alcohols will strongly interact with the carbonyl groups, whereas amide bases may interact preferentially with the amide NH. Although we are dealing with "solvent families" in the broadest sense, the empirical coordinate covalency ζ is not useful in this context.

In order to explore reasons for the correlation with α, we replotted Lay *et al.*'s data of the formal oxidation potential for ferrocene in alcoholic solvents[11b] and obtained a linear relationship between α and the E^o. However, the slope is significantly different from that observed for the ferrocenoyl-dipeptides **4**–**7**, suggesting that the peptide substitutent is modifying the redox potential of the Fc moiety by its interaction with the solvent. For ferrocenoyl-dipeptides in solvents with a very large HBD ability α, such as trifluoroethanol (α = 1.51) and 2-chloroethanol (α = 1.28), the electrode potential experiences a cathodic shift, indicating more facile oxidation of the Fc moiety and a net stabilization of Fe(III) over Fe(II). This change in E^o is related to the different strengths of interaction of each redox state with the solvent molecules.[21] The cathodic shifts of the electrode potentials that we observe on moving from solvents with small α to ones with large α indicate that the solvent molecules are more tightly bound for solvents with large α once the ferrocenoyl group is oxidized. This is consistent with the observations that the Fc^+ group will increase the acidity of the adjacent amide NH[23] and the ability of the Fc–C=O to become a stronger electron pair donor. In related ferrocenoyl-amidopyridine systems, protonation of the pyridine nitrogen, and thus formation of a cationic charge close to the Fc group, results in anodic shifts.[15h] Cathodic shifts were observed, however, when the ferrocenoylamidopyridine systems were studied in the presence of carboxylic acids.[15g] These cathodic shifts are believed[15g] to be a consequence of strong hydrogen bonding between the N–H of a ferrocenoyl-amidopyridine and the C=O of a carboxylic acid with the amide NH, as is proposed for Fc-peptides.

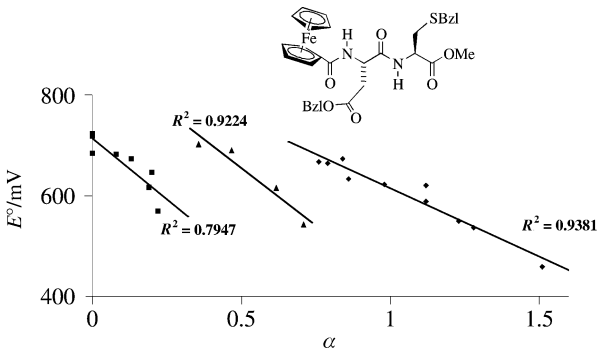

Fig. 1 Influence of the hydrogen bond donor ability α of various families of solvents on the redox potential of Fc-Asp(OBzl)-Cys(Bzl)-OMe (**7**): (◆) protic solvents (alcohols and acids); (▲) amides and N-bases; (■) others.

Table 4 Selected bond lengths (Å) and angles (°) for **8** · 1/3H_2O

C(1)–C(11)	1.471(2)	N–C(11)	1.328(2)
O(1)–C(13)	1.325(2)	N–C(12)	1.454(2)
O(2)–C(13)	1.205(3)	O(4)–C(15)	1.209(3)
O(3)–C(15)	1.322(2)	O(5)–C(11)	1.252(2)
C(11)–N–C(12)	121.68(16)	N–C(11)–C(1)	117.70(18)
O(5)–C(11)–N	121.77(17)	O(2)–C(13)–O(1)	125.16(18)
O(5)–C(11)–C(1)	120.52(18)	O(4)–C(15)–O(3)	123.42(19)

In this context, it is meaningful to interpret our results in terms of hydrogen bonding interactions of solvent molecules with the amide C=O of the Fc group and the peptide backbone. This is supported by NMR monitoring of additions of aliquots of methanol to a solution of **7** in $CDCl_3$, which showed large downfield shifts of the amide NH signal, indicative of H-bonding.[3] The presence or absence of H-bonding has effects on the electronic properties. Addition of solvents that will bond strongly with the amide C=Os or the ferrocenoyl C=O will cause changes in the electronic structure of the ferrocenoyl group. This in turn should influence the chemical shift of the hydrogens on the Fc group. The *ortho* hydrogens should be influenced the most due to their proximity to the peptide substitutent. In fact, addition of methanol causes shifts of the proton signals of the *ortho* hydrogens from δ 4.71 and 4.69 in neat $CDCl_3$ to δ 4.57 after the addition of methanol. The *meta* hydrogens and the hydrogens of the unsubstituted Cp are also shifted after the addition of methanol (from δ 4.34 to 4.24 for the meta hydrogens and from δ 4.20 to 4.05 for the protons of the unsubstituted Cp ring).

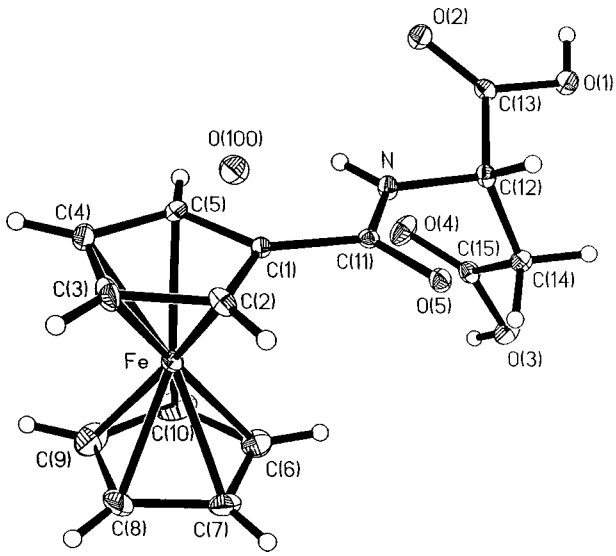

Fig. 2 ORTEP diagram for Fc-Asp(OH)-OH · 1/3H_2O (**8** · 1/3H_2O) showing a single molecule of **8** and the water molecule occupying a position allowing its interaction with CH(5) and the amide NH.

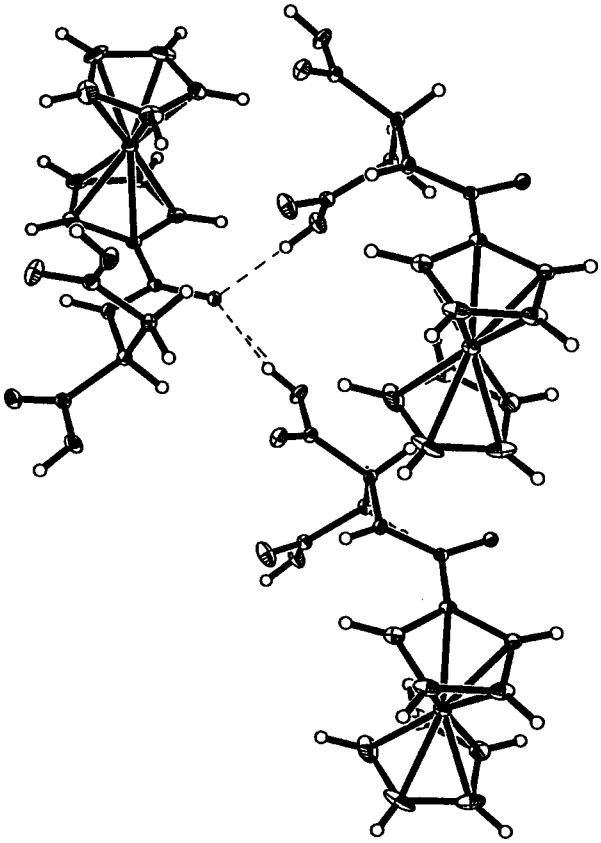

Fig. 3 ORTEP diagram for three adjacent molecules of **8** engaged in H-bonding. Two acid OH are H-bonded with the Fc–C=O group. The water molecule has been omitted for clarity.

Crystallographic studies

Indirect evidence of the ability of the Fc-dipeptide to form H-bonding interactions with solvents is provided by the X-ray crystal structure of **8**. Selected bond distances and angles are

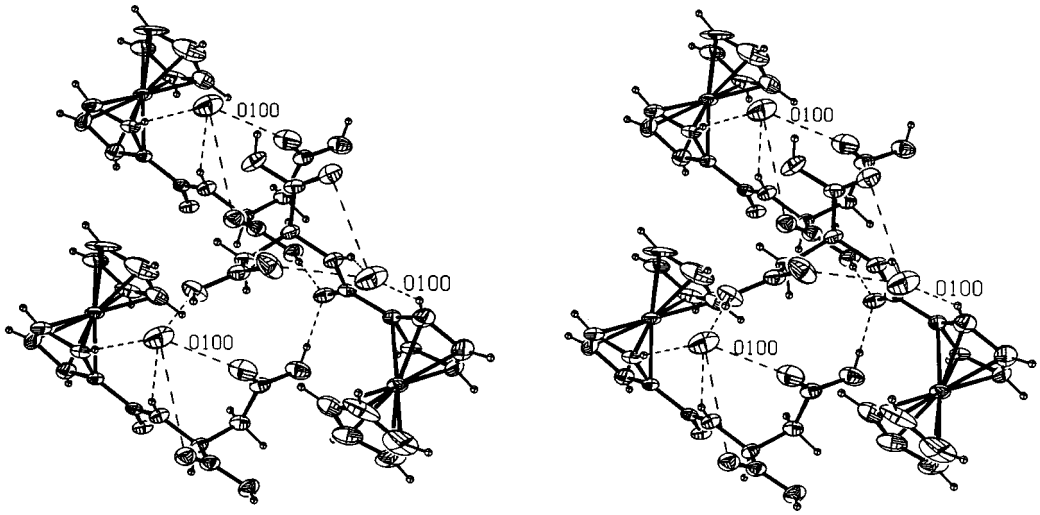

Fig. 4 Stereoscopic view of the extensive H-bonding network present in the solid state between the water molecule (O100) and three adjacent molecules of **8**. In addition to "conventional" O···H–N and O–H···O=C H-bonding, the water molecule is also involved in C–H···O interactions with the Cp ring.

summarized in Table 4 and an ORTEP[24] representation of **8** is shown in Fig. 2. The geometric features of **8** are similar to those of other Fc-peptides and Fc-amino acids.[25] The two Cp rings of the Fc group are parallel with a small bent angle[25] Cp–Fe–Cp of 1.1° and they adopt an eclipsed conformation. The amide and Cp groups are coplanar with a twist of only 3.4°, which is small compared to that seen in related systems.[25] Compound **8** crystallizes with 1/3 molecule of water, which occupies a position that enables H-bonding with the Fc-amide NH and the Asp–C=O groups. The Fc–C=O group is involved in hydrogen bonding interactions with the acid groups of the Asp acid side chain as well as the α-carboxyl group of two adjacent molecules, forming a bifurcated H-bond with O–H···O=C(Fc) contacts of 2.678(2) and 2.605(2) Å (Fig. 3). The H-bonding distance to the α-carboxy group is shorter, indicating a stronger H-bond, which is in line with the lower pK_a for this group ($pK_a = 1.88$) compared to the side chain carboxyl group ($pK_a = 3.65$).[26] Fig. 4 shows the extensive hydrogen bonding network involving the water molecule and three Fc-aspartic acid molecules. The water molecule is nestled in a pocket created by the Fc-aspartic acid moiety, which enables it to establish a series of H-bonding contacts. Unfortunately, we were not able to obtain crystals of the corresponding oxidized complex, which would enable us to directly compare the H-bonding abilities of the oxidized and reduced species.

Summary

Ferrocenoyl-dipeptides are readily synthesized from ferrocene carboxylic acid and various C-protected dipeptides. The ferrocenoyl-dipeptides each exhibit a reversible one-electron oxidation wave. The position of this oxidation wave is greatly dependent on the hydrogen bonding ability of the solvent, shows a correlation with the Kamlet–Taft parameter α, and exhibits a "solvent family" behavior. In general, an increase in the HBD ability α of the solvent causes a cathodic shift of the redox potential. However, it appears that other solvent effects, not yet accounted for, are influencing the redox potential. An X-ray study of Fc-Asp(OH)-OH shows a highly H-bonded structure, a result that suggests that the Fc-dipeptides would interact with H-bonding solvents. Solvent coordination most likely will involve the amide N–H and the carbonyl C=O, as was reported before.[2,3]

Acknowledgements

We thank the National Science and Engineering Research Council of Canada for financial support in the form of operating grants to H. B. K. (#218857-99) and J. W. Q. (#108071). M. V. B. thanks The University of Western Australia for a sabbatical leave. We thank Mr K. Thoms for the elemental analyses and MS measurements. We would also like to thank Dr R. S. Reid for discussions regarding multilinear regression analysis.

References

1 H.-B. Kraatz, D. M. Leek, A. Houmam, G. D. Enright, J. Lusztyk and D. D. M. Wayner, *J. Organomet. Chem.*, 1999, **589**, 38.
2 P. Saweczko and H.-B. Kraatz, *Coord. Chem. Rev.*, 1999, **190–192**, 185.
3 P. Saweczko, M.Sc. Thesis, University of Saskatchewan, 2001.
4 I. Bertini, H. B. Gray, S. J. Lippard and J. S. Valentine, *Bioinorganic Chemistry*, University Science Books, Mill Valley, CA, 1994.
5 (*a*) E. Fraga and G. R. Loppnow, *J. Phys. Chem. B*, 1998, **102**, 7659; (*b*) G. R. Loppnow and E. Fraga, *J. Am. Chem. Soc.*, 1997, **119**, 896; (*c*) M. A. Webb and G. R. Loppnow, *J. Phys. Chem. B*, 1998, **102**, 8923.
6 (*a*) E. M. Cilli, E. Oliveira, R. Marchetto and C. R. Nakaie, *J. Org. Chem.*, 1996, **61**, 8992; (*b*) M. Narita, J. S. Lee, S. Hayashi, Y. Yamazaki and Y. Sugiyama, *Bull. Chem. Soc. Jpn.*, 1993, **66**, 500; (*c*) M. Narita, J. S. Lee, S. Hayashi and M. Hitomi, *Bull. Chem. Soc. Jpn.*, 1993, **66**, 489; (*d*) M. Narita, J. S. Lee, S. Hayashi, Y. Yamazaki and M. Hitomi, *Bull. Chem. Soc. Jpn.*, 1993, **66**, 494; (*e*) M. Narita, S. Honda and S. Obana, *Bull. Chem. Soc. Jpn.*, 1989, **62**, 342; (*f*) M. Narita, H. Umeyama and T. Yoshida, *Bull. Chem. Soc. Jpn.*, 1989, **62**, 3582.
7 (*a*) M. Schaefer, C. Bartels and M. Karplus, *J. Mol. Biol.*, 1998, **284**, 835 and references therein; (*b*) H. Guo and M. Karplus, *J. Phys. Chem.*, 1994, **98**, 7104.
8 (*a*) A. Cammers-Goodwin, T. J. Allen, S. L. Oslick, K. F. McClure, J. H. Lee and D. S. Kemp, *J. Am. Chem. Soc.*, 1996, **118**, 3082; (*b*) D. S. Kemp, T. J. Allen, S. L. Oslick and J. G. Boyd, *J. Am. Chem. Soc.*, 1996, **118**, 4240; (*c*) D. S. Kemp, S. L. Oslick and T. J. Allen, *J. Am. Chem. Soc.*, 1996, **118**, 4249; (*d*) S. Shimizu and K. Shimizu, *J. Am. Chem. Soc.*, 1999, **121**, 2387.
9 H. A. O. Hill, *Coord. Chem. Rev.*, 1996, **151**, 115.
10 H. Shalev and D. H. Evans, *J. Am. Chem. Soc.*, 1989, **111**, 2667.
11 (*a*) R. L. Blackburn and J. T. Hupp, *J. Phys. Chem.*, 1990, **94**, 1788; (*b*) I. Noviandri, K. N. Brown, D. S. Fleming, P. T. Gulyas, P. A. Lay, A. F. Masters and L. Phillips, *J. Phys. Chem. B*, 1999, **103**, 6713.
12 M. J. Kamlet, J. L. M. Abboud, M. H. Abraham and R. W. Taft, *J. Org. Chem.*, 1983, **48**, 2877.
13 Y. Marcus, *Chem. Soc. Rev.*, 1993, 409.
14 (*a*) L. Engman, J. Persson, C. M. Anderson and M. Berglund, *J. Chem. Soc., Perkin Trans. 2*, 1992, 1309; (*b*) M. Jonsson, J. Lind, T. Reitberger, T. E. Eriksen and G. Merényi, *J. Phys. Chem.*, 1993, **97**, 11278; (*c*) M. Jonsson, J. Lind, G. Merényi and T. E. Eriksen, *J. Chem. Soc., Perkin Trans. 2*, 1995, 67; (*d*) M. Jonsson, D. D. M. Wayner and J. Lusztyk, *J. Phys. Chem.*, 1996, **100**, 17539.
15 (*a*) P. D. Beer, Z. Chen, A. J. Goulden, S. E. Stokes and T. Wear, *J. Chem. Soc., Chem. Commun.*, 1993, 1834; (*b*) P. D. Beer, Z. Chen, M. G. B. Drew, J. Kingston, M. Ogden and P. Spencer, *J. Chem. Soc., Chem. Commun.*, 1993, 1046; (*c*) P. D. Beer, *Chem. Commun.*, 1996, 689; (*d*) Z. Chen, A. R. Graydon and P. D. Beer, *J. Chem. Soc., Faraday Trans.*, 1996, **92**, 97; (*e*) P. D. Beer and M. Shade, *Chem. Commun.*, 1997, 2377; (*f*) P. D. Beer, A. R. Graydon, A. O. M. Johnson and D. K. Smith, *Inorg. Chem.*, 1997, **36**, 2112; (*g*) J. D. Carr, L. Lambert, D. E. Hibbs, M. B. Hursthouse, K. M. Malik and J. H. R. Tucker, *Chem. Commun.*, 1997, 1649; (*h*) J. D. Carr, S. J. Coles, W. W. Hassan, M. B. Hursthouse, K. M. A. Malik and J. H. R. Tucker, *J. Chem. Soc., Dalton Trans.*, 1999, 57.
16 (*a*) S. R. Hall, G. S. D. King and J. M. Stewart, *The XTAL 3.4 User's Manual*, University of Western Australia, Perth, Australia, 1995; (*b*) G. M. Sheldrick, SHELXL97, Program for the Refinement of Crystal Structures, Universität Göttingen, Göttingen, Germany, 1997.
17 J. Jones, *The Chemical Synthesis of Peptides*, Clarendon Press, Oxford, 1991.
18 A. Weisman, M. Gozin, H.-B. Kraatz and D. Milstein, *Inorg. Chem.*, 1996, **35**, 1792.
19 A. J. Bard and L. R. Faulkner, *Electrochemical Methods*, Wiley, New York, 1980.
20 R. Prins, A. R. Korswagen and A. G. T. G. Kortbeek, *J. Organomet. Chem.*, 1972, **39**, 335.
21 (*a*) C. D. Hall, N. W. Sharpe, I. P. Danks and Y. P. Sang, *J. Chem. Soc., Chem. Commun.*, 1989, 419; (*b*) J. C. Medina, T. T. Goodnow, S. Bott, J. L. Atwood, A. E. Kaifer and G. W. Gokel, *J. Chem. Soc., Chem. Commun.*, 1991, 290.
22 H.-B. Kraatz, *J. Organomet. Chem.*, 1999, **579**, 222.
23 M. H. Abraham, *Chem. Soc. Rev.*, 1993, **22**, 73.
24 C. K. Johnson, ORTEPII, Report ORNL-5138, Oak Ridge National Laboratory, Oak Ridge, TN, 1976.
25 L. Lin, A. Berces and H.-B. Kraatz, *J. Organomet. Chem.*, 1998, **556**, 11.
26 *CRC Handbook of Chemistry and Physics*, ed. D. R. Linde, 80th edn., CRC Press, Boca Raton, FL, 1999, sect. 7-1, 2.